Synthesis of Scroll-Type Composite Microtubes of Mo_2C/MoCO by Controlled Pyrolysis of $Mo(CO)_6$

Xiao-Lin Li and Ya-Dong Li*[a]

Abstract: Composite microtubes of Mo_2C/MoCO have been synthesized for the first time under well-controlled conditions by thermal decomposition of $Mo(CO)_6$ at about 600 °C. Here, thermal stability and phase transition of the products, as well as the influence of reaction temperature and argon flow rate, have been carefully investigated. All samples were characterized by X-ray powder diffraction (XRD), scanning electron microscopy (SEM), and X-ray photoelectron spectroscopy (XPS). The reaction model and rolling mechanism were proposed on the basis of the experimental facts.

Keywords: carbides · microtubes · molybdenum · scanning probe microscopy · X-ray diffraction

Introduction

One-dimensional (1D) tubular structures have attracted extensive interest over the past decade, because these fascinating systems are expected to have remarkable properties, and a wide range of potential applications.[1–2] Since the discovery of carbon nanotubes,[3] many techniques have been developed, and numerous tubular structures based on layered or nonlayered compounds, such as BN, $NiCl_2$, metal dichalcogenides (i.e., MoS_2, WS_2, NbS_2, TaS_2, TiS_2, ZrS_2, HfS_2, ReS_2), metal oxides (i.e., titanate, lanthanide hydroxide, VO_x, Ga_2O_3, $K_4Nb_6O_{17}$, $Mg_3B_2O_6$, $Al_{18}B_4O_{33}$), and Bi have been prepared.[4–16]

In contrast to the numerous literature published on the preparation of nano- or microtubules, only a few studies have been focused on the formation mechanism. On the basis of bending graphite sheets under high temperature or electron beam irradiation[17] and rolling phenomena (used for the synthesis of many nanotubes),[18–25] curving followed by seaming of molecular layers has been proposed to be responsible for the tube-formation process. In the synthesis of Bi, WS_2, MoS_2 nanotubes and W nanowires, we have found that 1D nanostructures can be obtained through the rolling of either a natural or an artificial lamellar structure.[16,19–21] Remskar and co-workers obtained direct evidence for the derivation of tubules from the bending of platelets.[22] Mallouk and Domen also provided clear evidence for the chemical transformation of lamellar oxides into tubular structures, and interpreted the layering of structures as a rolling process.[14,23] Recently, the rolling mechanism is further developed and some new tubular structures have been synthesized. Yada et al. reported the formation of tubular structures through the folding of flexible aluminium-based layers.[24] Kaner et al. reported the synthesis of carbon nanoscrolls by a chemical route.[25] A particularly important breakthrough in the rolling mechanism was the synthesis of SiGe nanotubes through the rolling of the pre-synthesized thin layers.[26]

The success of the rolling mechanism, and especially the synthesis of SiGe nanotubes, motivated us to probe the possibility of developing a method for the synthesis of tubular structures through the rolling of thin solid films. Our attention was drawn to thin films of molybdenum oxycarbides, which are easily obtained by the chemical vapor deposition method.

Molybdenum carbides and oxycarbides have received considerable interest due to their intrinsic mechanical properties, and potential applications in ceramic science and catalysis.[27–31] With a small particle size, carbide materials promise to allow the consolidation of fully dense solids with excellent fracture resistance for use as cutting tools, wear resistant parts, and high stress and temperature structural components.[27–28] As catalysts, molybdenum carbides and oxycarbides promise to be an inexpensive alternative to the noble metals with possibly even superior properties due to their ability to withstand high temperatures and resistance to poisoning.[29–30] Moreover, carbides with a microscopic hollow tubular structure have been developed as potential

[a] X.-L. Li, Prof. Y.-D. Li
Department of Chemistry
The Key Laboratory of Atomic & Molecular Nanosciences
Ministry of Education, Tsinghua University
Beijing, 100084 (P. R. China)
Fax: (+86) 10-6278-8765
E-mail: ydli@tsinghua.edu.cn

 DOI: 10.1002/chem.200305213

candidates for lightweight, thermal barrier, heat exchange materials, micro-sensors, electron emitter, electromagnetic absorbers, and so on.[31].

Herein, we have developed a simple method for the synthesis of scroll-type composite microtubes of Mo_2C/MoCO by controlled pyrolysis of $Mo(CO)_6$. As-synthesized microtubes have a diameter of about ten micrometers and a length up to millimeters long. Stability and phase transition of the products, as well as the influences of the reaction temperature and argon flow rate were investigated. On the basis of the experimental facts, the rolling mechanism was further developed. This strategy offers the possibility to further investigate tubular structured Mo_2C/MoCO, and may provide a general method for the growth of other microtubes. The rolling mechanism may become a general method for the synthesis of tubular structures.

Results and discussion

A series of representative scanning electron microscopy (SEM) images of as-synthesized microtubes are shown in Figure 1a–d. On the basis of SEM images, the tubular structures had a proportion of about 10% dispersed among numerous broken flakes. Large-scale synthesis of the microtubes by rolling might be difficult, however; by controlling the rate of temperature increase the proportion of microtubes reached 30%. (In an improved synthetic procedure, $MoCO_6$ samples were pushed into the hot zone at 300°C, and the furnace temperature was then increased to 600°C by a temperature programming procedure at the rate of 100°C per hour. The layer deposition and rolling procedure were well controlled). We believe that with better control of the factors, the proportion of microtubes might be further increased. Most of the microtubes had the scroll-type morphology with diameters of about ten micrometers and several millimeters in length. Figure 1a–c shows the representative scroll-type microtubes. The open ends and coiling patterns that were formed by the rolling process can be seen clearly in the figure. A high magnification SEM image (Figure 1d) provides further insight into the structure of individual microtubes, which consists of well-assembled uniform nanocrystalline products with diameters of about 30 nm.

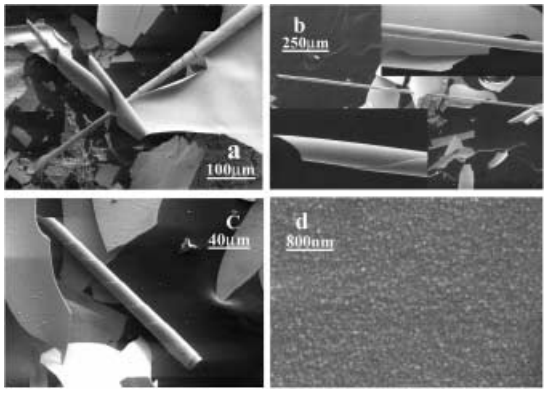

Figure 1. SEM images that show the as-synthesized microtubes. Typical scroll-type microtubes (a–c). High magnification image that shows the wall of the microtubes (d).

Figure 2 shows the typical XRD pattern of as-synthesized microtubes, in which the reflections have been attributed to two components, MoCO with the face-centered-cubic (fcc) structure, and Mo_2C with a hexagonal-closed-packed (hcp) structure. The reflection peaks at about $2\theta = 37.5°$, 43.6°, 63.6°, 76.1°, 80.4°, and 96.1° could be indexed to the (111), (200), (220), (311), (222), and (400) faces of fcc MoCO, with lattice constants of $a = 4.152$ Å (JCPDS card No: 17–0104). The reflections at $2\theta = 34.4°$, 38.0°, 39.4°, 52.2°, 61.6°, 69.6°, and 74.7° were indexed to (100), (002), (101), (102), (110), (103), and (112) faces of hcp Mo_2C with lattice constants: $a = 3.012$ Å and $c = 4.735$ Å (JCPDS card No: 35–0787). From the relative intensity of the peaks, we found that the fcc MoCO was the dominant phase.

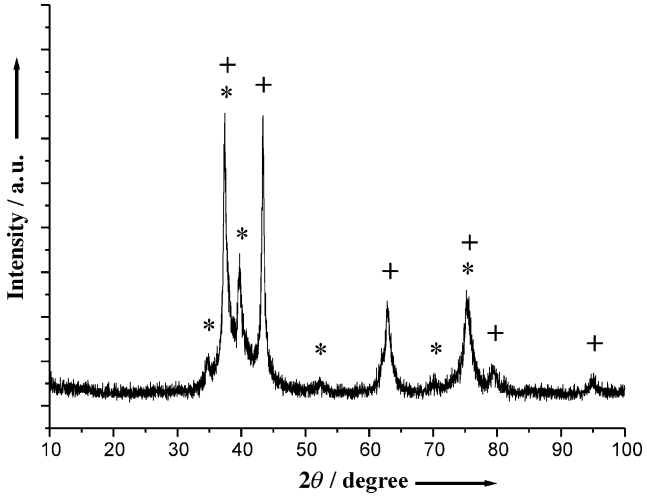

Figure 2. Typical XRD pattern of the microtubes obtained at 600°C. Mo_2C signal(*) and MoCO signal(+).

According to the literature,[32] the hcp Mo_2C contains no oxygen atoms. Thus the microtubes cannot be simply characterized as molybdenum oxycarbides. We believe that it was a kind of composite material of hcp Mo_2C and fcc MoCO with different amounts of amorphous carbon and oxygen intercalated in the structure. Energy dispersive X-ray spectroscopy (EDS) and X-ray photoelectron spectroscopy (XPS) were used to determine the composition of as-synthesized products.

EDS spectra for different microtubes, as well as different parts of the same microtube have been obtained. From all the spectra, it can be confirmed that the microtubes contained molybdenum, carbon, and a substantial amount of oxygen, which were in the molar ratio of about 0.26: 0.50: 0.24 (spectra is not shown).

XPS spectra of the Mo 3d, C 1s, and O 1s are shown in Figure 3, and correspond to the microtubes obtained at 600°C. The Mo 3d spectrum (Figure 3a) shows the presence of Mo 3d in several oxidation states located at 228.4 eV, 231.8 eV, and 235.0 eV. According to the literature,[33–34] the

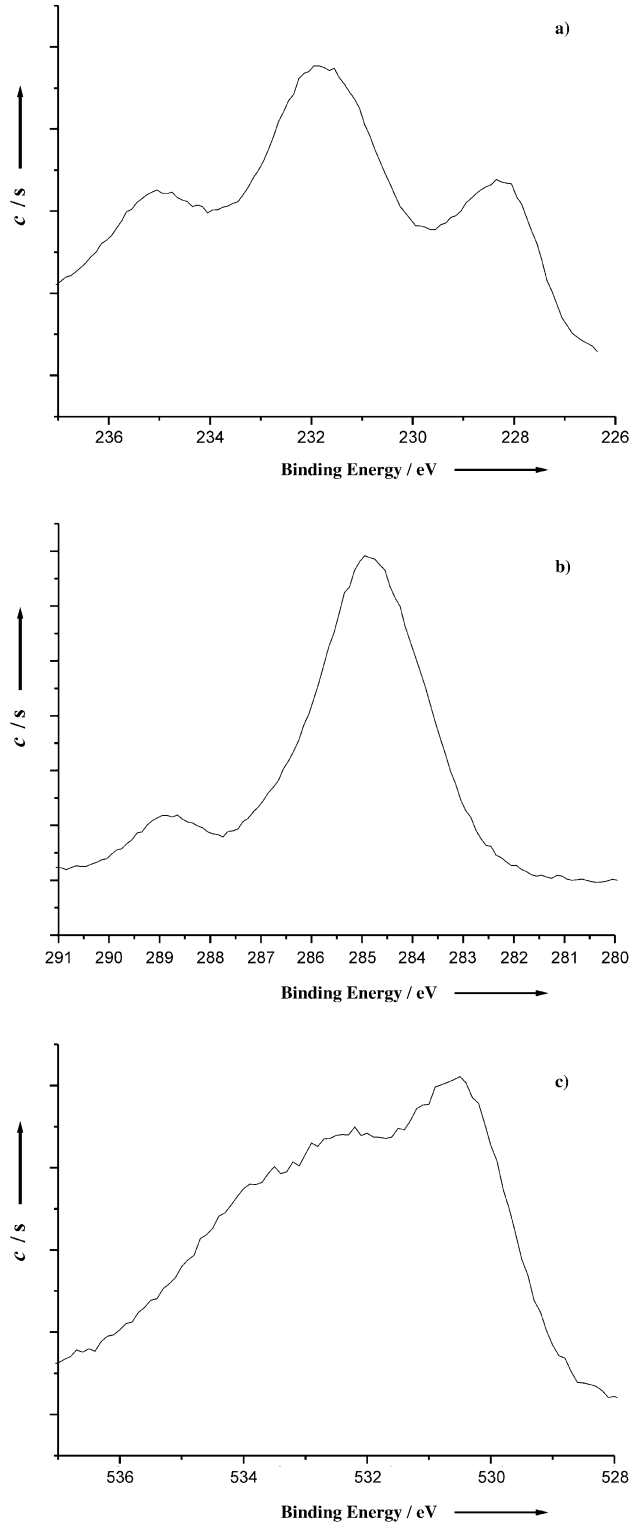

Figure 3. XPS spectra of Mo 3d, C 1s, and O 1s of the microtubes synthesized at 600 °C: a) Mo 3d, b) C 1s, and c) O 1s.

peak at 228.4 eV was unambiguously attributed to Mo atoms in the carbide form, and the peak at 235.0 eV was attributed to Mo^{6+}. The peak at 231.8 eV is probably due to the combination of three contributions of the oxycarbide phase, Mo^{4+} and Mo^{5+} species.[33–34] Figure 3b is the C 1s spectrum, which primarily shows two strong XPS peaks. The peak at 284.8 eV was attributed to amorphous carbon as reported by several authors.[33–34] The peak at 288.6 eV was attributed to the carbon atoms involved in carbonate species (C=O), and was due to contamination.[34] Further investigation revealed the weak signal at 283.5 eV may correspond to a carbon bonded to an oxygen atom and a metal in an oxycarbide form.[33–34] Because amorphous carbon formed by the pyrolytic reaction was accumulated on molybdenum carbides, the peak of C 1s at 284.8 eV was very strong. Thus, the carbon atom signal in the oxycarbide form was weak, and the signals for the carbon atoms in the carbide form could not be observed at all. The O 1s XPS spectrum also showed the presence of more than one peak. The peak located at 530.4 eV was attributed to the oxygen bonded to metal, while the peak at 532.8 eV was attributed to the oxygen atoms in the carbonate species.[33–34]

According to the XPS analysis, the molar ratio of Mo, C, and O was calculated to be about 0.22: 0.52: 0.26. Because the contamination by accumulated carbon and air could not be totally excluded, the amount of carbon and oxygen were a great deal larger.[32,33–34] According to the literature,[34] the signals of Mo^{IV}, Mo^{V}, and Mo^{VI} might also be ascribed to the exposition in air.

Spot analysis on a single microtube may provide valuable information on tubular materials. However, at this stage we could not carry out spot XRD analysis on a single microtube to determine the correct phase of the structure. Instead, we carried out EDS analysis on different microtubes, as well as, different parts of the same microtube to obtain spot analysis of the microtube composition. The EDS analysis showed that the tubular structures had almost the same composition of Mo, C, and O. TEM and ED analysis should be useful to reveal the local structure of the products. However, in our case, TEM and ED patterns provided the structure of random grind samples instead of the microtubes due to the following reasons: 1) The microtubes were only a small portion of the pyrolytic products; most were the broken sheets and 2) As-synthesized microtubes had diameters of about ten micrometers, and walls about several microns thick; they cannot be examined by TEM directly. The pyrolytic product must be grinded in order to be characterized by TEM. In the future, a suitable in-situ characterization technique is needed to conduct spot analysis on a single microtube to assign the correct phase of the tubular material.

Influence of the temperature: A series of experiments have been conducted for a better understanding of the pyrolytic reaction of $Mo(CO)_6$.

The influence of temperature was investigated from 200 °C to 800 °C. The results showed that microtubes could only be obtained at about 600 °C, although $Mo(CO)_6$ began to decompose at a rather low temperature. Figure 4 shows the typical XRD patterns of the samples obtained at 300–800 °C. From the XRD patterns, we determined that the decomposition reaction of $Mo(CO)_6$ was very complicated, and it was hard to obtain a single-phase product. The composition of the final products changed a great deal as the temperature increased. When the reaction temperature was below 500 °C,

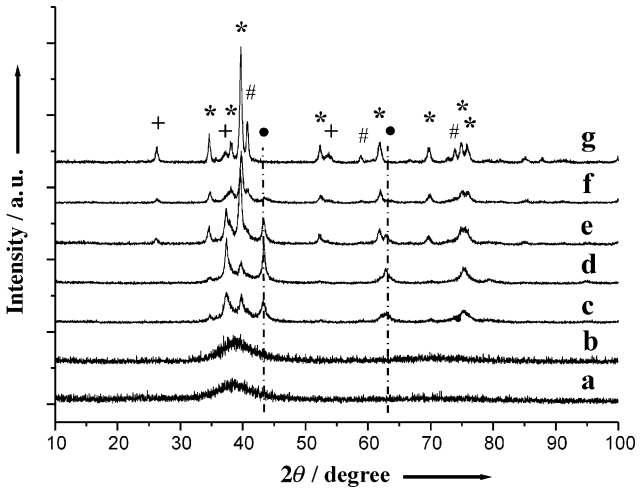

Figure 4. XRD patterns of the samples obtained at different reaction temperatures: a) 300 °C, b) 400 °C, c) 500 °C, d) 600 °C, e) 650 °C, f) 700 °C, and g) 800 °C. Mo_2C signal(*), MoO_2 signal (+), Mo signal(#), and MoCO signal(●).

only amorphous products were obtained. It was believed that the primary phase of the amorphous products was MoCO with certain amounts of accumulated amorphous carbon and oxygen. At 500 °C, nanocrystallines of fcc MoCO and hcp Mo_2C were obtained at the same time. With an increase in temperature, monoclinic MoO_2 (JCPDS card No: 76–1807) formed at about 650 °C. Body-centered-cubic (bcc) structured Mo metal formed when the temperature was higher than 700 °C. As shown in the image, reflection peaks at $2\theta = 40.6°$, 58.7°, 73.8°, and 87.7° could be an index to the (110), (200), (211), (220) faces of the bcc Mo, with lattice constants of $a = 3.147$ Å (JCPDS card No: 42–1120). Interestingly, the intensity of the fcc molybdenum oxycarbide decreased with increasing temperature. At 800 °C, signals of fcc MoCO completely disappeared. According to the XPS analyses, different amounts of amorphous carbon and oxygen might accumulate in the products at different temperatures. Thus, the molar ratio of Mo, C, and O of the products changed with the reaction temperature.

Morphology of the products obtained at all temperatures was characterized by SEM (SEM images are not shown). The results showed that different-sized flakes were obtained instead of microtubes. Those flakes had little difference in morphology, although the particle size grew larger with an increase in temperature.

A detailed reaction mechanism for the decomposition of $Mo(CO)_6$ will be discussed later.

The annealing time had little influence on the pyrolysis of $Mo(CO)_6$, because the pyrolytic reaction of $Mo(CO)_6$ was very fast. The composition and crystallinity of samples taken after five minutes of the reaction were almost the same as the products obtained after two hours.

Influence of the argon flow rate: In addition to the temperature, the argon flow rate had important influence on the structure of the products. Control experiments with argon flow rate from 10 to 100 sccm have been investigated. With a slow argon flow rate, for example 20 sccm, we obtained composite products of Mo_2C and MoCO in the hot zone. Careful investigation showed that small changes in the argon flow rate had little influence on the pyrolytic products, whereas the composition of the products changed when the argon flow rate greatly increased. When the argon flow rate was higher than 80 sccm, a white sublimation product of $Mo(CO)_6$ was obtained at the outlet of the quartz tube. $Mo(CO)_6$ vapor was quickly removed even before the decomposition. When the argon flow rate was about 50 sccm, the pyrolytic reaction of $Mo(CO)_6$ may have been responsible for the formation of black deposits at the downstream side, in which the temperature was about 80 °C. A representative XRD pattern of the black product is shown in Figure 5, in which all the reflection peaks were indexed to fcc MoCO. XPS characterization showed that Mo, C, and O were in the molar ratio of about 0.29: 0.37: 0.34.

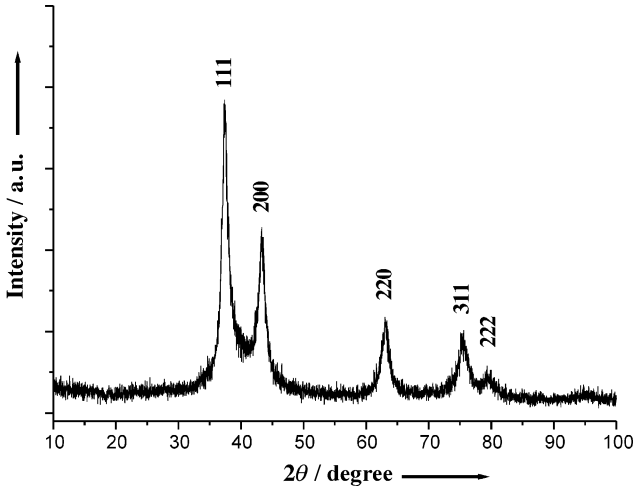

Figure 5. XRD pattern of the samples obtained at 80 °C with the argon flow rate at about 50 sccm.

Typical morphology of the as-synthesized MoCO crystalline products is shown in Figure 6, in which fibrous floccus and microspheres were found.

Decomposition reactions of $Mo(CO)_6$ at low temperature could only result in the formation of amorphous products. However, this strategy might provide a simple technique for the synthesis of MoCO crystalline products. Those crystallized MoCO samples had large surface areas, and their catalytic properties were under investigation.

It was believed that the quenching process caused by the high argon flow rate was the crucial factor in the formation

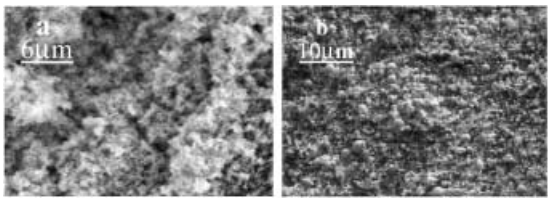

Figure 6. SEM images that show the typical morphology of MoCO crystalline products obtained at 80 °C with the argon flow rate at about 50 sccm.

of pure-phase MoCO crystalline products. During the thermal decomposition process, $Mo(CO)_6$ decomposed to form metallic Mo and CO vapors. With a low argon flow rate, Mo and CO might have further reacted at high temperature to yield Mo_2C, MoO_2, and Mo in addition to MoCO. When the argon flow rate was high, the formed Mo and CO vapors were quickly brought to the low temperature region, and reacted to form MoCO clusters. Those clusters further grew into MoCO crystalline products.

Thermal stability and phase transition of the products: As-synthesized microtubes were investigated by annealing the samples in a conventional tube-furnace from 600 to 800 °C. At high temperatures, the samples lost the tubular morphology and collapsed to different-sized flakes. The corresponding samples taken at 600 °C, 630 °C, 650 °C, 700 °C, and 800 °C were examined by XRD. The results (Figure 7) showed that

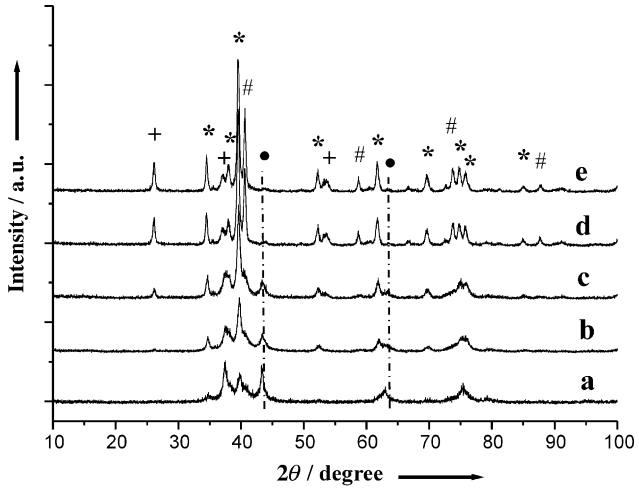

Figure 7. Thermal stability and phase transition of the microtubes obtained at 600 °C. XRD patterns of the samples annealed at: a) 600 °C, b) 630 °C, c) 650 °C, d) 700 °C, e) 800 °C. (Mo_2C signal(*), MoO_2 signal (+), Mo signal(#), and MoCO signal(●).

both the structure and composition of the microtubes changed remarkably with an increase in temperature. At 600 °C, fcc MoCO was the primary phase of the microtubes, and showed strong intensity in the XRD pattern. The intensity of MoCO decreased and completely disappeared at 800 °C. hcp Mo_2C always had a significant composition at all temperatures, and an increase in intensity was observed at high temperatures. MoO_2 was formed at 650 °C, and Mo was formed at 700 °C.

Thermal stability of the MoCO crystalline products obtained at 80 °C with high argon flow rate was also investigated. The samples were annealed to 800 °C. Typical XRD patterns of the samples taken at 80–800 °C are shown in Figure 8. The formation of MoO_2 was assigned at 600 °C. It was interesting to note that the relative intensity of Mo_2C and Mo of Figure 8e showed an important difference relative to Figure 7e.

From the literature[32–37] and our experiment results, we believe that the formation of MoO_2 and Mo might be ascribed to the decomposition of MoCO at high temperatures. A detailed reaction process will be discussed later.

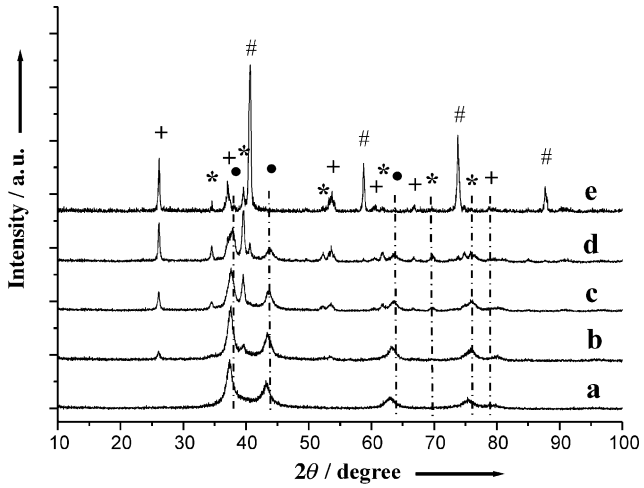

Figure 8. Thermal stability and phase transition of fcc MoCO obtained at 80 °C with a large argon flow rate. XRD patterns of samples annealed at: a) 80 °C, b) 600 °C, c) 650 °C, (d) 700 °C, and e) 800 °C. Mo_2C signal(*), MoO_2 signal(+), Mo signal(#), and MoCO signal(●).

Reaction mechanism: Thermal decomposition of $Mo(CO)_6$ has long been used to prepare metal films and molybdenum carbides.[35–37] However, due to the complexity of the subject, few studies have reported on the microscopic details of the reaction pathways. Singmaster et al. proposed that an intermediate product, such as $Mo(CO)_4$, had an important role in the photochemical decomposition of $Mo(CO)_6$,[35] whereas more authors believed that thermal decomposition of $Mo(CO)_6$ would cause the formation of metallic Mo and CO vapors.[36–37] Although the exact reaction pathway at the atomic scale cannot be solved at this stage, possible reaction mechanisms have been proposed on the basis of the literature[35–38] and our experimental results.

Reactions that may be involved in the pyrolysis of $Mo(CO)_6$ are expressed in Equations (1)–(5).

$$Mo(CO)_6 \rightarrow Mo + 6\,CO \quad (1)$$

$$Mo + CO \rightarrow MoCO \quad (2)$$

$$2\,CO \rightarrow C + CO_2 \quad (3)$$

$$Mo + 2\,CO \rightarrow MoO_2 + 2\,C \quad (4)$$

$$2\,Mo + 2\,CO \rightarrow Mo_2C + CO_2 \quad (5)$$

At low temperatures, the reaction was simple and MoCO was formed as the main product, whereas at high temperatures, various reactions may have taken place at the same time; this results in the formation of several kinds of products such as MoCO, Mo_2C, MoO_2, and Mo.

Investigations on the thermal stability of the products showed that MoCO was not stable at high temperatures and might have decomposed to form Mo_2C, MoO_2, and Mo.[36] The reactions involved are shown in Equations (6) and (7).

$$4\,MoCO \rightarrow 2\,MoO_2 + Mo_2C + 3\,C \quad (6)$$

$$MoCO \rightarrow Mo + CO \quad (7)$$

Rolling mechanism: The concept that scrolling may lead to the formation of tubular structures has long been known.[17–18] However, it was not until very recently that the rolling mechanism has been proposed as a general mechanism for the synthesis of nanotubes. Up to now, there is a lot of literature on the rolling mechanism.[17–26] From the literature[17–26] and our experimental facts, we believe that the formation of the Mo_2C/MoCO microtubes could be ascribed to the rolling mechanism.

In addition to the typical scroll-type microtubes shown in Figure 1, extensive and careful SEM observations are shown in Figure 9, which further confirms that as-synthesized microtubes were formed by the rolling process. Direct evidence for the rolling mechanism has been found in the half-tube and half-plate structure, as shown in Figure 9a and b. Figure 9a shows the image of a scroll-type microtube with one end wound. Figure 9b shows the coexistence of microtubes and rolling sheets in the same structure. The polycrystalline thin film appears to roll at the edges of each sheet. Figure 9c shows two parallel scrolls, that were formed by the rolling of a single sheet. The discovery of this phenomenon provides unassailable evidence to support the rolling mechanism. Samples at different rolling stages are shown in Figures 9d–f. Following the rolling sequence, shown in Figures 9d–f, tubular structures are believed to have been formed.

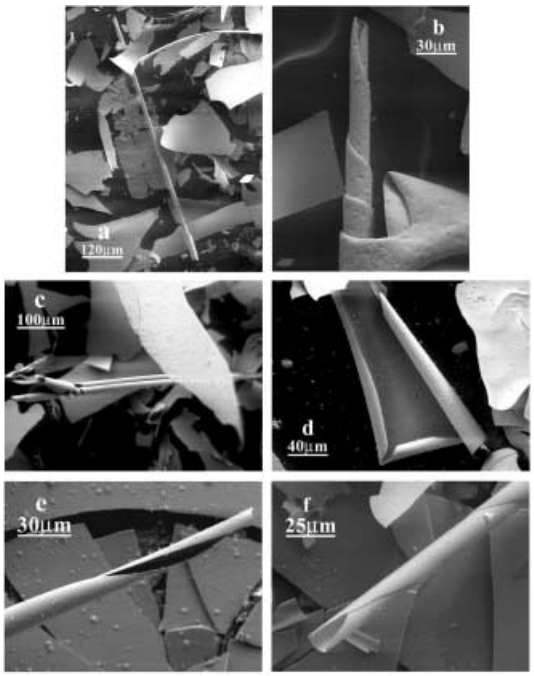

Figure 9. SEM images that give evidence of the rolling process for the formation of microtubes: a) microtube with the wound end, b) half-tube/half-sheet in the same structure, c) two parallel tubes formed by the rolling of one sheet, and d)–f) samples obtained at different rolling stages.

The novel rolling mechanism for the formation of composite microtubes from the polycrystalline films requires a clear understanding. Thermal stress, electron irradiation, intercalation, sonochemical treatments, and others have been suggested to perhaps initiate the rolling of molecular layers.[17–25] Recently, thin solid films of SiGe have been rolled up into nanotubes, because of the lattice mismatch between the solid film and the substrate.[26] In this case, the driving force for the curling of the thin solid films could be ascribed to 1) the mismatch between the deposition film and quartz glass substrate and 2) the interaction between the assembled nanoparticles of the film. Under appropriate conditions, the interaction between the film and the substrate could be reduced, because of the lattice mismatch, while keeping the interactions of assembled nanocrystallines of the film; thus causing the thin layer to wrap and fold back on itself. Scroll-type tubular structures were formed through the rolling of the thin films.

No tubular structures were formed in control experiments carried out at temperatures higher than 600 °C, because the driving force was not adequate. The crystalline products that formed at high temperatures had large particle sizes. Films composed of large-sized particles could not grow very large, and might have easily cracked during the rolling process. Elemental composition of the film was also believed to have a certain influence on the formation of microtubes. A detail investigation is in progress.

Our experiments have shown an example of the rolling mechanism to synthesize micrometer-scale tubular structures through the rolling of solid thin films. Analogous to this method, a variety of functional materials can be engineered to produce solid-state tubular structures. It is foreseeable that scrolling may become a general method for the synthesis of other tubular structures.

Conclusion

To summarize, we have developed a simple method for the synthesis of composite microtubes of Mo_2C/MoCO under well-controlled conditions by the pyrolysis of $Mo(CO)_6$. Thermal stability of the products, as well as the influence of the reaction temperature and argon flow rate, have been investigated. The pyrolytic reaction model was discussed on the basis of literature and our experimental results. The rolling mechanism was further developed and applied to the formation of micrometer-scale tubular structures. This synthetic strategy offers the possibility for further investigation of tubular structures of Mo_2C/MoCO, and may become a general method for the growth of nano- and microtubes.

Experimental Section

Synthesis of microtubes: The typical synthesis procedure for the formation of microtubes was carried out in a conventional tube furnace at about 600 °C with the argon flow rate at about 20 sccm (standard cubic centimeter per minute). $Mo(CO)_6$ (0.3 g) was loaded in a quartz boat and quickly pushed into the hot zone of the furnace at a stable temperature of about 600 °C. Quartz glass substrates were used to collect the deposi-

tion. After calcination at 600 °C for two hours, the system was cooled to room temperature under argon, and silver-gray products were obtained on the quartz glass substrate.

Characterization: Powder X-ray diffraction (XRD) was performed on a Bruker D8-advance X-ray diffractometer with CuK_α radiation ($\lambda =$ 1.54178 Å). The 2θ range used in the measurement was from 10° to 100° in steps of 0.02° with a count time of 1 s. The size and morphology of as-synthesized samples were determined by using a LEO-1530 SEM with an accelerating voltage of 20 kV. The composition of the products was characterized by using a PHI-5300 ESCA XPS.

Acknowledgement

This work was supported by NSFC (20025102, 50028201, 20151001), the Foundation for the Author of National Excellent Doctoral Dissertation of P. R. China, and the state key project of fundamental research for nanomaterials and nanostructures.

[1] a) C. Dekker, *Phys. Today* **1999**, *52*, 22 – 28; b) R. Tenne, A. K. Zettl, *Top. Appl. Phys.* **2001**, 80, 81 – 112.
[2] G. R. Patzke, F. Krumeich, R. Nesper, *Angew. Chem.* **2002**, *114*, 2554 – 2571; *Angew. Chem. Int. Ed.* **2002**, *41*, 2446 – 2461.
[3] S. Iijima, *Nature* **1991**, *354*, 56 – 58.
[4] N. G. Chopra, R. J. Luyren, K. Cherry, V. H. Crespi, M. L. Cohen, S. G. Louis, A. Zettl, *Science* **1995**, *269*, 966 – 967.
[5] Y. R. Hachohen, E. Grunbaum, J. Sloan, J. L. Hutchison, R. Tenne, *Nature* **1998**, *395*, 336 – 337.
[6] a) R. Tenne, L. Margulis, M. Genut, G. Hodes, *Nature* **1992**, *360*, 444 – 446; b) Y. Feldman, E. Wasserman, D. J. Srolovitz, R. Tenne, *Science* **1995**, *267*, 222 – 225.
[7] M. Nath, C. N. R. Rao, *J. Am. Chem. Soc.* **2001**, *123*, 4841 – 4842.
[8] a) M. Nath, C. N. R. Rao, *Angew. Chem.* **2002**, *114*, 3601 – 3604; *Angew. Chem. Int. Ed.* **2002**, *41*, 3451 – 3454; b) J. Chen, Z. L. Tao, S. L. Li, *Angew. Chem.* **2003**, *115*, 2197 – 2201; *Angew. Chem. Int. Ed.* **2003**, *42*, 2147 – 2151.
[9] a) M. Brorson, T. W. Hansen, and C. J. H. Jacobsen, *J. Am. Chem. Soc.* **2002**, *124*, 11582 – 11583; b) K. S. Coleman, J. Sloan, N. A. Hanson, G. Brown, G. P. Clancy, M. Terrones, H. Terrones, M. L. H. Green, *J. Am. Chem. Soc.* **2002**, *124*, 11580 – 11581.
[10] X. M. Sun, Y. D. Li, *Chem. Eur. J.* **2003**, *9*, 2229.
[11] a) X. Wang, Y. D. Li, *Angew. Chem.* **2003**, *115*, 3135 – 3138; *Angew. Chem. Int. Ed.* **2003**, *26*, 3027 – 3030; b) X. Wang, Y. D. Li, *Adv. Mater.* **2003**, *17*, 1442 – 1445.
[12] a) M. E. Spahr, P. Betterli, R. Nesper, M. Miiller, F. Krumeich, H. U. Nissen, *Angew. Chem.* **1998**, *110*, 1339 – 1342; *Angew. Chem. Int. Ed.* **1998**, *37*, 1263 – 1265; b) F. Krumeich, H. J. Muhr, M. Niederberger, F. Bieri, B. Schnyder, R. Nesper, *J. Am. Chem. Soc.* **1999**, *121*, 8324 – 8331; c) M. Niederberger, H. J. Muhr, F. Krumeich, F. Bieri, D. Gunther, R. Nesper, *Chem. Mater.* **2000**, *12*, 1995 – 2000.
[13] S. Sharma, M. K. Sunkara, *J. Am. Chem. Soc.* **2002**, *124*, 12288 – 12 293.
[14] a) G. B. Saupe, C. C. Waraksa, H. N. Kin, Y. J. Han, D. M. Kaschak, D. M. Skinner, T. E. Mallouk, *Chem. Mater.* **2000**, *12*, 1556 – 1562; b) R. E. Schaak, T. E. Mallouk, *Chem. Mater.* **2000**, *12*, 3427 – 3434.
[15] a) R. Z. Ma, Y. Bando, D. Golberg, T. Sato, *Angew. Chem.* **2003**, *115*, 1880 – 1882; *Angew. Chem. Int. Ed.* **2003**, *42*, 1836 – 1838; b) R. Z. Ma, Y. Bando, T. Sato, C. C Tang, F. F. Xu, *J. Am. Chem. Soc.* **2002**, *124*, 10668 – 10669.
[16] Y. D. Li, J. W. Wang, Z. X. Deng, Y. Y. Wu, X. M. Sun, D. P. Yu, P. D. Yang, *J. Am. Chem. Soc.* **2001**, *123*, 9904 – 9905.
[17] a) R. D. Heidenreich, W. M. Hess, L. L. Ban, *J. Appl. Crystallogr.* **1968**, *1*, 1; b) D. Ugarte, *Nature* **1992**, *359*, 707 – 709.
[18] a) R. Bacon, *J. Appl. Phys.* **1960**, 31, 283 – 290; b) S. Amelinckx, D. Bernaerts, X. B. Zhang, G. Van. Tendeloo, J. Van. Landuyt, *Science* **1995**, *267*, 1334 – 1338; c) O. Zhou, R. M. Fleming, D. W. Murphy, C. H. Chen, R. C. Haddon, A. P. Ramirez, S. H. Glarum, *Science* **1994**, *263*, 1744 – 1747.
[19] Y. D. Li, X. L. Li, R. R. He, J. Zhu, Z. X. Deng, *J. Am. Chem. Soc.* **2002**, *124*, 1411 – 1416.
[20] X. L. Li, Y. D. Li, *Chem. Eur. J.* **2003**, *9*, 2 – 7.
[21] Y. D. Li, X. L. Li, Z. -X. Deng, B. C. Zhou, S. S. Fan, J. W. Wang, X. M. Sun, *Angew. Chem.* **2002**, *114*, 343 – 345; *Angew. Chem. Int. Ed.* **2002**, *41*, 333 – 335.
[22] a) M. Remskar, Z. Skraba, F. Cleton, R. Sanjines, F. Levy, *Appl. Phys. Lett.* **1996**, 69, 351 – 353; b) M. Remskar, Z. Skraba, M. Regula, C. Ballif, R. Sanjines, F. Levy, *Adv. Mater.* **1998**, *10*, 246 – 249; c) M. Remskar, Z. Skraba, R. Sanjines, F. Levy, *Appl. Phys. Lett.* **1999**, 74, 3633 – 3635.
[23] a) R. Abe, K. Shinohara, A. Tanaka, M. Hara, J. Kondo, K. Domen, *J. Mater. Res.* **1998**, *13*, 861 – 865; b) R. Abe, K. Shinohara, A. Tanaka, M. Hara, J. Kondo, K. Domen, *Chem. Mater.* **1997**, *9*, 2179 – 2184.
[24] M. Yada, H. Hiyoshi, K. Ohe, M. Machida, T. Kijima, *Inorg. Chem.* **1997**, *36*, 5565 – 5569.
[25] L. M. Viculis, J. J. Mack, R. B. Kaner, *Science* **2003**, *299*, 1361.
[26] O. G. Schmidt, K. Eberl, *Nature* **2001**, *410*, 168.
[27] J. M. Giraudon, L. Leclercq, G. LeclercQ, A. Lofberg, A. Frennet, *J. Mater. Sci.* **1993**, *28*, 2449 – 2454.
[28] M. Kmetz, S. L. Suib, F. S. Galasso, *J. Am. Ceram. Soc.* **1989**, *72*, 1523 – 1524.
[29] a) R. B. Levy, M. Boudart, *Science* **1973**, *181*, 547 – 549; b) T. C. Xiao, A. P. E. York, V. C. Williams, H. Al-Megren, A. Hanif, X. Y. Zhou, M. L. H. Green, *Chem. Mater.* **2000**, *12*, 3896 – 3905; c) J. B. Claridge, A. P. E. York, A. J. Brungs, C. M. arquez-Alvarez, J. Sloan, S. C. Tsang, M. L. H. Green, *J. Catal.* **1998**, *180*, 85 – 100.
[30] a) C. Bouchy, C. Phamhuu, B. Heinrich, C. Chaumont, M. J. Ledoux, *J. Catal.* **2000**, *190*, 92 – 103; b) M. J. Ledoux, P. D. Gallo, C. Phamhuu, A. P. E. York, *Catal. Today* **1996**, *27*, 145 – 150; c) E. A. Blekkan, C. Phamhuu, M. J. Ledoux, J. Guille, *Ind. Eng. Chem. Res.* **1994**, 33, 1657 – 1664.
[31] S. Motojima, W. In-Hwang, H. Iwanaga, *J. Mater. Sci.* **2001**, *36*, 673 – 677.
[32] a) A. Hanif, T. C. Xiao, A. P. E. York, J. Sloan, M. L. H. Green, *Chem. Mater.* **2002**, *14*, 1009 – 1015; b) S. T. Oyama, P. Delporte, C. Phamhuu, M. J. Ledoux, *Chem. Lett.* **1997**, 9, 949 – 950; c) J. S. Lee, L. Volpe, F. H. Ribeiro, M. Boudart, *J. Catal.* **1988**, *112*, 44 – 53.
[33] a) P. Delporte, F. Meunier, C. Phamhuu, P. Vennegues, M. J. Ledoux, J. Guille, *Catal. Today* **1995**, *23*, 251 – 267; b) T. Miyao, I. Shishikura, M. Matsuoka, M. Nagai, *Chem. Lett.* **1996**, 7, 561 – 562.
[34] a) P. Delporte, C. Phamhuu, M. J. Ledoux, *Appl. Catal. A* **1997**, 149, 151 – 180; b) M. J. Ledoux, C. Phamhuu, J. Guille, H. Dunlop, *J. Catal.* **1992**, *134*, 383 – 398.
[35] a) I. F. Ferguson, J. B. Hinseough, D. Morse, A. W. Miller, *Nature* **1964**, 202, 1327 – 1328; b) K. A. Singmaster, F. A. Houle, R. J. Wilson, *J. Phys. Chem.* **1990**, *94*, 6864 – 6875.
[36] a) C. C. Cho, S. L. Bernasek, *J. Appl. Phys.* **1989**, 65, 3035 – 3043; b) I. M. Watson, J. A. Connor, R. Whyman, *Polyhedron* **1989**, *8*, 1794 – 1796.
[37] W. J. Wei, M. H. Lo, *Appl. Organomet. Chem.* **1998**, *12*, 201 – 220.
[38] *Gmelins Handbuch der Anorganischen Chemie*, Gmelin-Institut für Anorganische Chemie, Springer, Heidelberg.

Received: June 10, 2003
Revised: September 15, 2003 [F5213]

